

# Dynamic compression of non-ideal argon plasma

V. E. Bespalov, V. K. Gryaznov, A. N. Dremin, and V. E. Fortov

*Division of Institute of Chemical Physics, USSR Academy of Sciences*

(Submitted June 27, 1975)

*Zh. Eksp. Teor. Fiz.* **69**, 2059–2066 (December 1975)

Experimental results are presented on the investigation of the equation of state of a non-ideal argon plasma obtained with an explosive shock tube. The registration of the shock-wave front velocity, of the plasma density, and of the plasma temperature made it possible to obtain  $P$ - $V$ - $H$ - $T$  information on the thermodynamic properties of the shock-compressed plasma. The obtained data are compared with theories of a non-ideal plasma; it is noted that bound states make an appreciable contribution.

PACS numbers: 52.25.Kn, 52.35.Lv

## 1. INTRODUCTION

The design and development of many modern high-energy devices (laser heating, magnetocumulation and MHD generators, various pinches, etc.<sup>[1-3]</sup>) entail the use of a dense plasma under conditions of strong inter-particle interaction. The possibilities of a consistent theoretical investigation of such a medium are limited by the small parameters of the interaction and by the difficulties in choosing the pseudopotential when solving the problem by the Monte Carlo method.<sup>[4]</sup>

The main difficulties in the experimental study of a non-ideal plasma are the need for high energy densities in a medium of appreciable density. The temperatures and pressures that develop in this case greatly exceed, as a rule, the heat-endurance limits of the apparatus materials, so that the experiments must be performed in pulsed regimes at high power levels. To investigate the thermodynamic properties of non-ideal media, particular promise is offered by dynamic methods<sup>[5,6]</sup> based on supplying the energy to the investigated substance through viscous dissipation of energy in the front of a shock wave. An additional advantage of these methods, for media with limited diagnostics capabilities, is the use of the conservation laws on the discontinuity front,<sup>[6]</sup> which make it possible to connect the experimentally registered hydrodynamic characteristics of the shock-discontinuity propagation with the thermodynamic properties of the shock-compressed medium and deduce from them a thermodynamically complete equation of state.<sup>[6,7]</sup> The use of the shock-wave technique in high-pressure physics has made it possible to measure the thermodynamic<sup>[5]</sup> and optical<sup>[8]</sup> properties of condensed media at extremely high pressures and temperatures. Experiments on dynamic compression of saturated Cs vapor<sup>[9]</sup> have made it possible to investigate the equation of state of a nondegenerate plasma at appreciable interaction parameters and to raise the question of its phase composition. At the same time, the interpretation of the obtained data<sup>[9]</sup> within the framework of model equations of state<sup>[10]</sup> has pointed to an appreciable contribution of the discrete spectrum to the thermophysical characteristics of the system. This circumstance makes it necessary to perform experiments with other chemical elements in as large a range of parameters as possible, calling for a large increase in the energy ratings of the experimental apparatus.

We present here the results of an experimental investigation of the equation of state of a non-ideal argon plasma by a dynamic method based on compression and irreversible heating of argon gas in the front of a high-power ionizing shock wave. The experiments were per-

formed with an explosive shock tube in which the propelling gas was made up of the detonation products of a high-power condensed explosive.

## 2. PLASMA GENERATION AND DIAGNOSTICS

Thermodynamic calculations of the parameters of the argon plasma produced behind the front of a flat stationary shock wave<sup>[11]</sup> have yielded the optimal (in the sense of an appreciable deviation of the plasma from ideal) experimental conditions, corresponding to a shock-wave velocity  $(7-9) \times 10^5$  cm/sec. To realize this range of parameters, a non-ideal plasma generator was developed,<sup>[12]</sup> in the form of a glass shock tube of inside diameter 5 cm and working-section length 25–30 cm. A shock wave of the required intensity was produced by expanding the detonation products of hexogen (a condensed explosive with a per-unit energy content  $\sim 10^4$  J/cm<sup>3</sup>, in argon compressed beforehand to a pressure  $P_0$ ). The flow of the shock-compressed plasma in the generator was made one-dimensional and quasi-stationary by suitable choice of the dimensions of the active explosive charge and of the conditions of its initiation, and also by inertial containment of the plasma against lateral expansion by the massive glass walls of the shock-tube channel. The power of the experimental apparatus was  $\sim 10^{11}$  W at a total energy release  $\sim 3 \times 10^6$  J.

The shock-wave front velocity  $D$  in the argon was measured by an electric-contact-base method and by an optical method, with accuracy  $\sim 1-1.5\%$ . Within the limits of this error, the ionization front coincides with the shock-wave luminescence front.

The density  $\rho = V^{-1}$  of the shock-compressed plasma was determined by a pulsed x-ray method<sup>[13]</sup> in which x radiation passing through the plasma was registered. The effective wavelength of this radiation was chosen from considerations of maximum sensitivity and minimum statistical measurement error<sup>[13]</sup>, and amounted to 0.7–0.3 Å at initial argon pressures  $P_0 = 2-15$  bar. The x-ray source was a BSV-9 tube (see Fig. 1) operating, to increase the intensity, in a forced regime with a pulse current up to 0.3 A produced by discharge of a capacitor bank through the tube. The measurement section of the shock tube was an organic-glass insert ring with ionization pickups and two-millimeter windows for the x-rays, covered with beryllium foil. To ensure an acceptable time resolution ( $\sim 10^{-7}$  sec), the width of the x-ray beam was additionally limited by lead diaphragms. The radiation passing through the plasma was registered with an FEU-29 photomultiplier with NaI scintillator. To protect the measurement circuit from damage by the air shock wave and by fragments, the x-ray tube and the detector

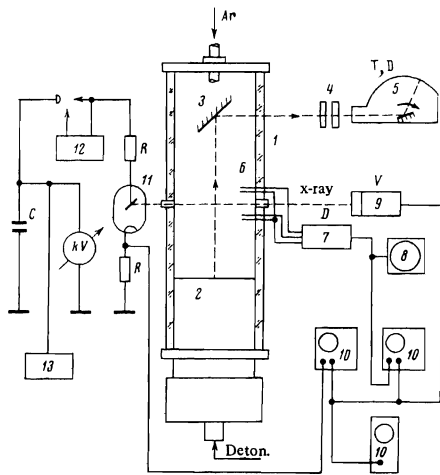


FIG. 1. Experimental setup: 1—shock tube, 2—active explosive charge with detonation lens, 3—mirror, 4—interference filter with attenuator, 5—SFR-2m high-speed moving-image camera, 6—electric-contact velocity pickups, 7—pickup power supply, 8—OK-15 oscilloscope with spiral sweep, 9—x-ray receiver (NaI scintillator, photomultiplier, and cathod follower), 10—recording oscillographs, 11—x-ray tube, 12—discharge-gap control block, 13—generator unit.

system were located  $\sim 1$  meter away from the explosive generator and were shielded by a strong steel structure. A typical oscillogram of the plasma density profile is shown in Fig. 2; one can see the sharp shock-wave front and the region of the homogeneous moving plasma "plug." The accuracy with which the density was registered was determined from the x-ray pictures of the shock waves at low initial pressure (weak deviation of the plasma from ideal) and amounted to  $\sim 8\%$ .

In view of the instabilities that occur at the instant of ignition of the controlled air-filled discharge gap and during the initial operation of the x-ray tube, the active explosive charge was detonated and the recording apparatus triggered through appropriate delay lines, using a special high-voltage electric detonator with precise operating times. Special electric decoupling circuits were used to suppress the electric static induced during the instant of the explosion and when the high-voltage x-ray apparatus was turned on.

The temperature of the shock-compressed plasma was measured by a brightness method<sup>[14,15]</sup> based on measuring the intensity of the optical radiation emitted by the plasma. The brightness temperature of the shock-compressed plasma was determined by photometric comparison of the density of photographic film on which the glow of the shock wave and light from standard sources were time-scanned with an SFR-2M high-speed moving-image camera.

The standards were an FPK-50 lamp, with brightness temperature  $T = 8600 \pm 200^\circ \text{K}^{(1)}$  and an ÉV-45 capillary flash with a black-body-radiation temperature  $T = 39000 \pm 700^\circ \text{K}$  in the range 2000–8000 Å. When the standard source was photographed, a stepped neutral attenuator<sup>[15]</sup> was mounted on the focal arc of the SFR-2M camera, making it possible to cover the entire photographic density range expected in the photography of the shock front. Inasmuch as the object and the standard were photographed under identical conditions, there was no need to use the reciprocity law to determine the temperature.<sup>[15,16]</sup> To exclude the effect of the photochemical development on the measurement results, the films of

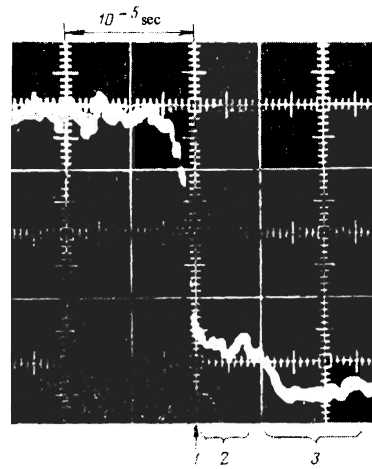


FIG. 2. X-ray pattern of density profile: 1—shock-wave front, 2—shock-compressed plasma, 3—detonation products.

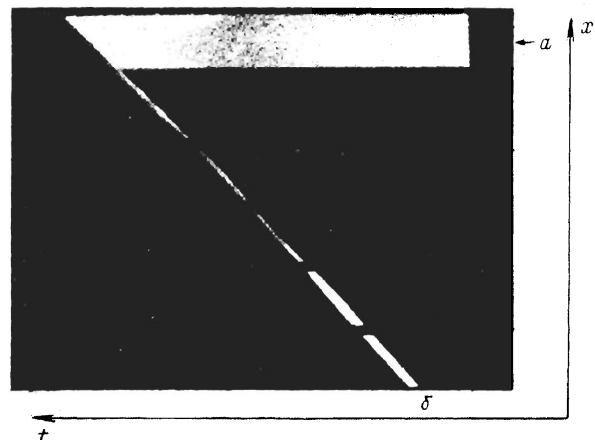


FIG. 3. Streak photograph of the experiment: a) scan of the radiation from the shock-wave front, b) trajectory of plasma motion: the reference markers are spaced 2.5 cm apart.  $P_0 = 5$  atm.

each run of experiments and the standard photographs were developed simultaneously.

The optical registration scheme is clear from Fig. 1. A flat stationary mirror placed at the end of the shock tube at  $45^\circ$  to its axis produced an image in the form of a longitudinal scan (a in Fig. 3), from which the plasma brightness temperature was measured. In the experiments, the longitudinal axis of the explosive shock tube was placed parallel to the rotation axis of the SFR-2M mirror, so that the time position of the plasma could be registered, and the shock-wave front velocity could be determined from the slope of its trajectory (b in Fig. 3).

Most measurements were made at an effective wavelength  $5800 \pm 50 \text{ \AA}$ , which was separated with an interference filter. To ensure operation in the linear section of the characteristic curve of the photographic films, calibrated neutral filters were used. The accuracy with which the temperature was determined was estimated by recording the radiation of shock-compressed air, for which, in view of the small deviation of the plasma from ideal, there are reliable thermodynamic calculations<sup>[17]</sup> and detailed measurements.<sup>[14,15]</sup> The results of the experiments, and also the data on the control series of measurements of the temperature of an argon plasma at

a wavelength  $4950 \pm 50 \text{ \AA}$  allow us to estimate the temperature error at 5–7%.

### 3. EXPERIMENTAL RESULTS

The use of the shock-wave technique in high-pressure physics is based on the connection between the kinematic characteristics of the motion of the shock discontinuity and the thermodynamic properties of the shock-compressed medium, as established by the mass, momentum, and energy conservation laws<sup>[6]</sup>:

$$P = P_0 + \rho_0 D^2 (1 - \rho_0 / \rho_1), \quad H = H_0 + D^2 (1 - \rho_0^2 / \rho_1^2) / 2, \quad (1)$$

which make it possible, given the initial conditions (labeled by the subscript zero) and the measured front velocity  $D$  and measured density  $\rho$ , to determine in each experiment the pressure  $P$  and the enthalpy  $H$  of the medium behind the shock-discontinuity front. We note that terms corresponding to radiant energy transport have been left out of (1), since their role is usually small<sup>[6]</sup>; concrete estimates for argon are given in<sup>[11]</sup>.

It follows from (1) that<sup>[9]</sup> the pressure and enthalpy of strongly-compressed media are determined in practice by the shock-wave front velocity  $D$ —the quantity most readily and accurately measured in dynamic experiments. For this reason, the best choice for the second independent parameter in dynamic investigations of the equation of state of gaseous media is the directly registered shock-compression density. Measurements of  $D$  and of  $\rho = V^{-1}$  at various initial conditions and shock-wave intensities make it possible, in accord with (1), to determine the caloric equation of state of the shock-compressed plasma,  $H = H(P, V)$ , in the phase-diagram region covered by the Hugoniot adiabats.<sup>[7]</sup> Since  $H$  is not a thermodynamic potential with respect to the variables  $P$  and  $V$ , to obtain a thermodynamically closed equation of state we need<sup>[7]</sup> the additional relation  $T = T(P, V)$ . The temperatures listed in the table were obtained by averaging 3–5 experiments for each  $P_0$ . The employed experimental procedure makes it possible to monitor the optical thickness of the shock-compressed plasma by watching the increase of the radiation intensity with time.<sup>[14]</sup> In all the experiments, the optical thickness was outside the limits of the resolution of the SFR-2M camera, and at any rate it did not exceed  $10^{-1}$  cm, so that the shock wave could be regarded as an absolutely black surface radiator in the employed spectral intervals.

The results of the temperature measurement may be distorted by the presence, in front of the shock wave, of a layer of gas heated by the short-wave radiation of the shock-compressed plasma.<sup>[6]</sup> However, a theor-

etical<sup>[6, 18]</sup> and experimental<sup>[17, 19]</sup> study of the screening of the radiation of the strong shock waves shows that this effect manifests itself, starting with  $D \sim 12 \times 10^5$  cm/sec,<sup>[19]</sup> and decreases with increasing initial pressure of the argon. A special series of experiments, in which radiation emerging at  $45^\circ$  to the shock-wave front was registered,<sup>[15]</sup> has shown that there is no noticeable optical screening under our conditions.

The experiments were performed in the range of initial pressures  $P_0 = 2\text{--}15$  bar, determined by the minimal and almost complete absorption of the x rays in the plasma. The range of velocities  $D$  realized in the experiments was close to optimal<sup>[12]</sup> and was determined by the energy capabilities of the employed explosive.

Let us estimate the expected experimental error. The error in the measurement of  $P_0$  and  $T_0$  is of the order of 1% and results in an approximate error of 1.5% in  $\rho_0$ . An error in  $D$  on the order of 1.5% and in  $\rho$  on the order of 8% yield, in accordance with (1)

$$\begin{aligned} \delta P &= [(\delta \rho_0)^2 + 4(\delta D)^2 + (\sigma - 1)^{-2}(\delta \rho)^2]^{1/2} \sim 4\%, \\ \delta H &= [4(\delta D)^2 + (\sigma^2 - 1)^{-2}(\delta \rho)^2]^{1/2} \sim 3\%. \end{aligned}$$

When the experimental results are compared with the theories of plasma non-ideality, the quantities  $P$  and  $H$  are treated as independent variables, and the entire error is assigned to  $\rho$ :

$$\delta \rho_H = \delta V_H \sim [(\delta P)^2 + (\delta H)^2 + (\delta \rho_0)^2]^{1/2} \sim 10\%.$$

At fixed  $P$  and  $T$  we have  $\delta \rho_T = \delta V_T \sim 12\text{--}13\%$ .

The measurement results are given in the table, where they are compared with the Debye theory in the small canonical ensemble of statistical mechanics. The calculated values are given for fixed  $P$  and  $H$  (the comparison with experiment is with respect to  $V$  and  $T$ ) or at fixed  $P$  and  $T$  (comparison with respect to  $V$  and  $H$ ). Figure 4 shows, for two characteristic experimental points, a more detailed comparison of the experimental thermodynamic data (labeled 1 in the sections of the figure—the error corridor is shaded) with the following theories and models:

2—Idealized approximation. The Planck-Larkin convergent quantum-mechanical expression was used for the partition functions of the bound state.<sup>[20, 10]</sup>

$P_0$ , bar	Experiment					Debye theory					
	$D \cdot 10^{-4}$ , cm/sec	$V_1$ , cm <sup>3</sup> /g	$P \cdot 10^{-3}$ , bar	$H \cdot 10^{-10}$ , erg/g	$T \cdot 10^{-3}$ , K	$P, H = \text{const}$			$P, T = \text{const}$		
						$V$	$T$	$\Gamma$	$n_0 \cdot 10^{-20}$ , cm <sup>-3</sup>	$V$	$H$
2	7.55	39.1	1.63	28.0	23.0	35.22	22.36	1.28	1.57	37.04	30.42
2	7.5	41.4	1.59	27.6	23.0	35.62	22.17	1.27	1.5	35.15	26.94
2	7.5	41.8	1.59	27.6	22.0	35.62	22.17	1.27	1.5	35.15	26.94
5	6.5	20.5	2.88	20.5	18.3	16.91	20.76	1.66	2.11	14.22	14.25
5	6.5	20.7	2.88	20.5	18.3	16.91	20.76	1.66	2.11	14.22	14.25
5	6.6	19.4	3.0	21.2	18.5	16.47	21.0	1.7	2.29	13.83	14.66
7	6.15	17.86	3.45	18.1	17.2	13.3	20.03	1.77	2.14	10.94	11.87
7	6.2	17.5	3.52	18.4	17.2	13.08	20.13	1.79	2.24	10.72	11.85
7	6.2	16.3	3.59	18.6	17.2	12.9	20.23	1.82	2.33	10.51	11.84
10	5.7	14.3	4.15	15.4	16.0	10.26	19.06	1.84	1.99	8.342	9.924
10	6.2	12.6	5.0	18.4	18.0	9.112	20.32	2.18	3.39	7.902	12.95
10	5.8	10.1	5.0	16.4	16.6	8.703	19.54	2.09	2.77	7.20	10.67
15	5.25	9.66	5.17	13.0	15.6	7.645	18.04	1.88	1.77	6.497	9.343
15	5.3	8.09	5.54	13.5	17.0	7.26	18.33	2.0	2.10	6.666	11.21
15	5.4	7.72	5.81	14.1	17.4	7.014	18.57	2.10	2.41	6.519	11.77

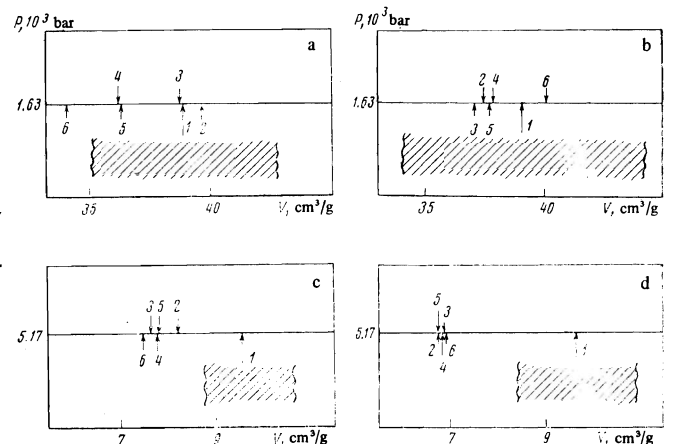


FIG. 4. Comparison of experiment with non-ideal plasma theories (the notation is explained in the text) for the caloric (a, b) and thermal (c, d) equations of state: a)  $P_0 = 2$  atm,  $H = 28 \times 10^{10}$  erg/g, b)  $P_0 = 15$  atm,  $H = 13 \times 10^{10}$  erg/g, c)  $P_0 = 2$  atm,  $T = 23 \times 10^3$  K, d)  $P_0 = 15$  atm,  $T = 15.6 \times 10^3$  K.

3—Debye theory with small canonical ensemble.<sup>[10]</sup>

4—Debye theory with grand canonical ensemble.<sup>[10]</sup>

5—Normalized Debye approximation for a singly-ionized plasma<sup>[17]</sup> (the condition of local electroneutrality is satisfied for an arbitrary charge.<sup>[22, 23]</sup>

6—Monte Carlo calculations of the null model of a plasma with pseudopotential  $\epsilon = 2$  (see<sup>[24]</sup> for details), where, in addition, the null method is compared with other variants of the Monte Carlo calculation.

At low pressures and densities, the results of the experiments correspond to the theoretical approximations. The discrepancy increases with increasing density and exceeds decisively the expected experimental errors at  $P_0 = 7-15$  bar. An interpretation of the results shows that in the investigated range of parameters, at constant  $H$  and  $T$ , the pressure of a non-ideal partly-ionized plasma exceeds the ideal-gas value, and this excess increases upon compressure. The corrections for the interaction in the continuous spectrum, obtained from the self-consistent theories<sup>[10]</sup> are insufficient for the description of the obtained experimental material. By introducing into the equation of the ionization equilibrium and additional decrease of the ionization potential it is possible to increase the number of free charges and consequently the kinetic part of the pressure, but such an operation decreases the value of the enthalpy and leads to an even greater deviation from experiment for the caloric equation of state<sup>[9]</sup>.

Calculations based on model equations of state<sup>[10, 25]</sup> have shown that a noncontradictory description of experiment can be obtained in principle by taking into account the contribution made to the thermodynamics of the system by the deformation of the energy levels of the bound electrons, due to the strong interparticle interaction—an effect usually ignored in thermodynamic calculations.<sup>[6, 10]</sup> A description of phenomena of this type calls for complicated self-consistent quantum-mechanical calculations.<sup>[25]</sup>

In the investigated range of parameters, no abrupt discontinuities of the thermodynamic functions were registered at all, nor any qualitative hydrodynamic anomalies<sup>[26]</sup> that might be interpreted as first-order phase transitions in a non-ideal plasma.<sup>[4]</sup>

We are deeply grateful to A. A. Leont'ev, B. N. Lomakin, and V. E. Chertoprud for help with the optical measurements.

<sup>1)</sup>The flash lamp was calibrated beforehand by a photoelectric method at the working wavelength, using a standard incandescent ribbon lamp (SI 8-200).

<sup>1)</sup>R. Physics of High Energy Density, ed. by P. Caldorola and H. Knoepfel, Academic, 1971.

<sup>2)</sup>J. G. Linhart, Nucl. Fusion **10**, 3 (1970).

<sup>3)</sup>J. Nickoll, L. Wood et al., Nature **239**, 139 (1972).

<sup>4)</sup>G. E. Norman and A. N. Starostin, Teplofiz. Vys. Temp. **8**, 413 (1970).

<sup>5)</sup>L. V. Al'tshuler, Usp. Fiz. Nauk **85**, 197 (1965) [Sov. Phys. Usp. **8**, 52 (1965)].

<sup>6)</sup>Ya. B. Zel'dovich and Yu. P. Raizer, Fizika udarnykh voln i vysokotemperaturnykh gidrodinamicheskikh yavlenii (Physics of Shock Waves and High-Temperature Hydrodynamic Phenomena), Nauka, 1966.

<sup>7)</sup>V. E. Fortov and Yu. G. Krasnikov, Zh. Eksp. Teor. Fiz. **59**, 1645 (1970) [Sov. Phys.-JETP **32**, 897 (1971)].

<sup>8)</sup>S. B. Kormer, Usp. Fiz. Nauk **94**, 641 (1968) [Sov. Phys. Usp. **11**, 229 (1968)].

<sup>9)</sup>B. N. Lomakin and V. E. Fortov, Zh. Eksp. Teor. Fiz. **63**, 92 (1972) [Sov. Phys.-JETP **36**, 48 (1973)]; Dokl. Akad. Nauk SSSR **206**, 576 (1972) [Sov. Phys. Dokl. **17**, 889 (1973)].

<sup>10)</sup>V. E. Fortov, B. N. Lomakin, and Yu. G. Krasnikov, Teplofiz. Vys. Temp. **9**, 869 (1971).

<sup>11)</sup>V. K. Gryaznov, I. L. Iosilevskii, and V. E. Fortov, Zh. Prikl. Mekh. Tekh. Fiz. **3**, 70 (1973).

<sup>12)</sup>V. E. Fortov, Yu. V. Ivanov, A. N. Dremin, V. K. Gryaznov, and V. E. Bespalov, Dokl. Akad. Nauk SSSR **221**, 1307 (1975) [Sov. Phys. Dokl. **20**, 295 (1975)].

<sup>13)</sup>B. N. Lomakin and V. E. Fortov, Teplofiz. Vys. Temp. **9**, 1291 (1971).

<sup>14)</sup>I. Sh. Model', Zh. Eksp. Teor. Fiz. **32**, 714 (1957) [Sov. Phys.-JETP **5**, 589 (1957)].

<sup>15)</sup>Yu. A. Zatsepin, E. G. Popov, and M. A. Tsikulin, Zh. Eksp. Teor. Fiz. **54**, 112 (1968) [Sov. Phys.-JETP **27**, 63, (1968)].

<sup>16)</sup>A. S. Dubovik, Fotograficheskaya registratsiya bystro-protekayushchikh protsessov (Photography of Fast Processes), Nauka, 1964.

<sup>17)</sup>N. M. Kuznetsov, Termodinamicheskie funktsii i udarnye adiabaty vozdukh pri vysokikh temperaturakh (Thermodynamic Functions and Shock Adiabats of Air at High Temperatures), Mashinostroenie, 1965.

<sup>18)</sup>Yu. P. Raizer, Zh. Eksp. Teor. Fiz. **32**, 1528 (1957) [Sov. Phys.-JETP **5**, 1242 (1957)].

<sup>19)</sup>Yu. N. Kisilev and B. D. Khristoforov, Fizika goreniya i vzryva **10**, 116 (1974).

<sup>20)</sup>A. I. Lapkin, Zh. Eksp. Teor. Fiz. **38**, 1896 (1960) [Sov. Phys.-JETP **11**, 1363 (1960)].

<sup>21)</sup>V. K. Gryaznov and I. L. Iosilevskii, Chislennye metody mekhaniki sploshnoi sredy **4**, 166 (1973).

<sup>22)</sup>G. A. Martynov, Zh. Eksp. Teor. Fiz. **54**, 159 (1968) [Sov. Phys.-JETP **27**, 87 (1968)].

<sup>23)</sup>F. H. Stillinger and R. Lowett, J. Chem. Phys. **49**, 1991 (1968).

<sup>24)</sup>B. V. Zelener, G. É. Norman, and V. S. Filinov, Teplofiz. Vys. Temp. **10**, 1160 (1972).

<sup>25)</sup>V. K. Grjasnov, A. I. Ivanova, and V. E. Fortov, Int. Conf. on Phenomena in Ionized Gases, Eindhoven, 1975.

<sup>26)</sup>V. E. Fortov, Teplofiz. Vys. Temp. **10**, 168 (1972).

Translated by J. G. Adashko  
221